PHYSICOCHEMICAL DIFFERENCES BETWEEN FRAGMENTS OF PLASMA MEMBRANE AND ENDOPLASMIC RETICULUM

DONALD F. HOELZL WALLACH, VIRENDRA B. KAMAT, and MITCHELL H. GAIL

From the Department of Biological Chemistry, Harvard Medical School, Boston, Massachusetts

ABSTRACT

Specific turbidities, densities, and refractive indices of fragments of plasma membrane (PM) and endoplasmic reticulum (ER) from Ehrlich ascites carcinoma have been measured. A spherical shell model of specified dimensions and refractive index was established for PM fragments. The ionic composition of the dispersion medium was varied systematically. Increases in $\Gamma/2$ caused increases in the turbidity of both PM and ER suspensions, the greatest effects being observed with Ca^{2+} and Mg^{2+}. In the case of PM this effect is attributable mainly to aggregation, whereas "structural" changes account for most of the turbidity increase with ER. The pH was also varied systematically to obtain pH- density and turbidity profiles and to establish the isoelectric pH of the two membrane types (PM—3.6; ER—4.35). Turbidity was maximum at "isoelectric" pH, which corresponds in each case to the region of minimum charge on the particle surfaces. Both PM and ER show large increases of density at the "isoelectric" pH, but only ER shows substantial structurally based turbidity increase under these conditions. Both PM and ER show operation of electrostatic attractions near "isoelectric" pH. PM has been shown to have ionically distinctive inner and outer surfaces while ER shows no such dissymmetry. The necessary theoretical background for interpretation of turbidity and density measurements is included, as well as a discussion of the limitations of our conclusions and the biological importance of our results.

The membrane components of Ehrlich ascites carcinoma (EAC) microsomes are fluid-filled vesicles arising primarily from the disrupted endoplasmic reticulum and the fragmented plasma membrane of these cells (1–5). They can be fractionated by ultracentrifugal methods into four distinct membrane classes (3, 5, 6): namely, (1) "rough" endoplasmic reticulum; (2) vesicles—here designated *ER*—arising primarily from the "smooth" endoplasmic reticulum; (3) vesicles—here designated *PM*—originating primarily from the plasma membrane of the intact cell; and (4) particles, of unknown origin, physiochemically related to—but immunologically distinct from—PM and separated from the latter by virtue of their lower density. These particles are referred to here as the density (ρ) 1.025 component.

We are examining in detail the distinguishing chemical, physical, and immunologic features of the above membrane classes and now report on some of the light-scattering properties of PM- and ER-type vesicles. In particular, we describe the distinctive absorbance changes which follow alterations of the ionic environment of these par-

ticles and which reflect events occurring within individual vesicles, and also provide evidence as to specific surface properties of the two vesicle types.

MATERIALS AND METHODS

Preparation of Membrane Components

Ehrlich ascites carcinoma microsomes were separated as described previously (5, 6) into a crude "plasma membrane" (PM) fraction and an "endoplasmic reticulum" (ER)–ribosome fraction by use of discontinuous Ficoll density gradients containing 0.001 M Mg^{2+} and 0.001 M Tris-HCl (pH 8.6).

The crude PM fraction was then separated into a low density component ($\rho = 1.025$) and the purified PM component ($\rho = 1.045$) by ultracentrifugal equilibration in Ficoll gradients as described before (5, 6). Prior to turbidimetric measurements it is necessary to remove the membrane components from Ficoll, since this substance has an appreciable turbidity of its own. Although both the 1.025 membranes and the PM membranes can be sedimented by dilution of the Ficoll followed by ultracentrifugation, firm pellets can be obtained only at $\Gamma/2 > 0.1$ or in the presence of polyvalent cations. The following procedure was found satisfactory for the preparation of these membrane components for turbidimetric studies:

The two fractions were diluted 1:5 with 0.01 M Tris-HCl (pH 8.6), containing $CaCl_2$ to a final concentration of 0.01 M, and were centrifuged at 39,000 RPM for 30 min (Spinco SW 39 rotor manufactured by Spinco Division of Beckman Instruments, Belmont, California). The pellets were then suspended to a concentration of about 5 mg protein/ml in 0.01 M Tris-HCl (pH 8.6), 0.01 M EDTA. Excess EDTA and EDTA metal complexes were removed by dialysis against 400 volumes of 0.001 M Tris-HCl (pH 8.6) or by passage of the suspension through Sephadex G-25 previously equilibrated against 0.001 M Tris-HCl (pH 8.6).

ER membranes were prepared as follows: the ER-ribosome fraction was first freed from trapped PM material by a repetition of the Ficoll-Mg gradient procedure. The sediment, containing ER and ribosomes, was then suspended in 0.01 M EDTA, 0.01 M Tris (pH 8.6) and dialyzed first against 100 volumes of the same buffer, followed by two sequential 1-hr dialyses against 100 volumes of 0.001 M Tris (pH 8.6). The suspension, now free of aggregates, was layered on top of sucrose of $\rho = 1.16$ containing 0.001 M Tris (pH 8.6) and centrifuged at 25,000 RPM (SW 25 rotor) for 3 hr. The layer which accumulated at the density barrier, containing ER membranes free of ribosomes, was collected and stored at −28°C. For turbidimetric measurements, the material is diluted to $\rho = 1.025$ with 0.001 M Tris (pH 8.6) and centrifuged at 39,000 RPM for 30 min (Spinco SW 39 rotor). The pellet was resuspended in 0.001 M Tris (pH 8.6) to a concentration of 1 to 2 mg protein/ml.

To determine the variation in the total density of PM particles with pH, the membranes were mixed into Ficoll gradients of identical density range, but buffered to different pH values at $\Gamma/2 = 0.01$. The buffers were those used for the pH-absorbance profiles. The gradients were centrifuged at 39,000 RPM for 16 hr at 4°C (Spinco L-2 preparative ultracentrifuge, SW 39 rotor). The tubes were then cut into ten fractions and the proteins and densities of each fraction determined as before (4). Unimodal density distributions were obtained. The data are presented as the % change of modal density, using the density at pH 8.2 as reference value.

Wet volume per mg protein was measured by packing membrane particles into calibrated capillaries. This was done in polycarbonate adaptors for Spinco SW 39 tubes. The adaptors have a conical space at the top leading smoothly into a capillary 1 mm diameter and 2 cm long. The adaptors, containing about 0.5 ml membrane suspension (about 2 mg protein), were centrifuged until the pellet had attained constant height (45 min) as measured microscopically. Protein determinations were then done on pellets and supernatants. Over 90% of the applied protein was recovered in the pellets. Specific volumes were calculated in terms of pellet volume per mg pellet protein. Specific volumes, determined in triplicate, agreed to within 7%. (Details of the procedure will be published separately.)

Turbidity Measurements

Turbidity was measured using a Beckman DU monochromator (Beckman Instruments Inc., Fullerton, California) with a Gilford Model Absorbance Indicator (Gilford Instrumentation Lab., Oberlin, Ohio). The latter was provided with a blackened, tubular aperture (2-mm diameter; 10-mm length) placed so that the semiacceptance angle of the photomultiplier was about 2°. Under these conditions, the detector views the primary beam and only little of the scattered light, and the specific extinction is invariant with concentration up to a particle concentration of about 0.4 mg protein/ml (Fig. 1). At higher particle concentrations, collection of scattered light by the detector leads to underestimates of turbidity. For this reason, measurements were restricted to absorbance values of 0.600 or less.

Matched 1-cm and 10-cm cuvettes were employed. The cuvette compartment was thermostated at 25°C. Measurements of absorbance on each filling of the cuvettes were done in triplicate (except in kinetic experiments) and were reproducible to 0.001 absorbance units: usually the readings were identical.

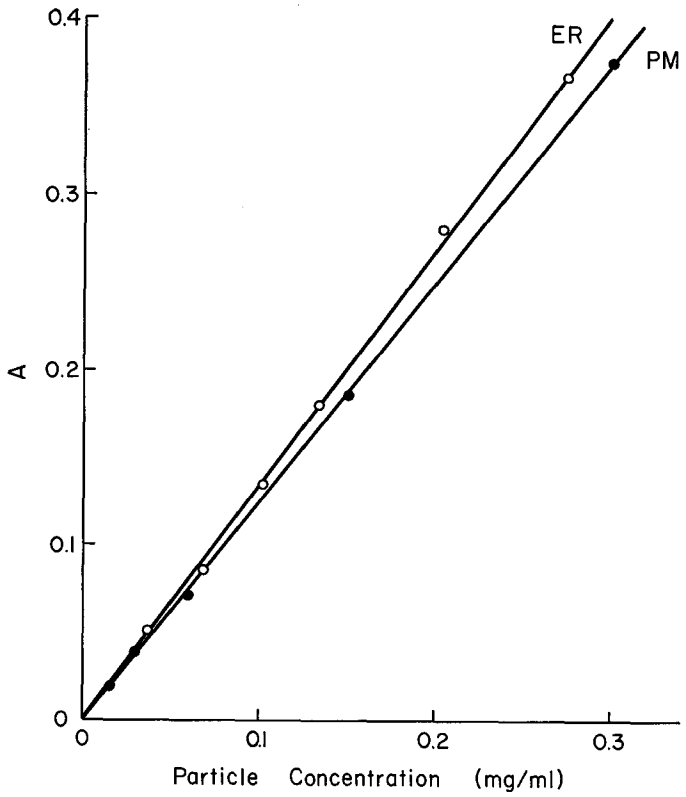

FIGURE 1 Variation of the absorbance of PM and ER suspensions with particle concentration. $\lambda = 400$ mμ. Buffer, 0.001 M Tris-HCl (pH 8.2). Particle concentration is in terms of membrane "protein."

Turbidities are expressed in terms of specific absorbance, $\frac{A}{C}$, defined as the absorbance, in general eral at 400 mμ, of a dispersion with protein concentration C μg/ml (where C is 100 μg/ml, except in concentration studies).

Turbidity changes either are given directly or are expressed in terms of Δ, the *fractional absorbance increment*, defined as

$$\Delta = (A - A_O)/A_O$$

where A_O is the absorbance at concentration C, under standard conditions, namely at 400 mμ, 25°C, atmospheric pressure, and with 0.001 M Tris-HCl, pH 8.2, as dispersion medium. A is the absorbance of the same dispersion under "altered" conditions.

In general, Δ is a function of the parameters of the "altered condition" as well as the concentration C. However, aggregation experiments, in which the effects of pH and other ionic changes are being studied, are carried out at constant protein concentration ($C = 100$ μg/ml). In this case

$$\Delta = \frac{(A/C) - (A_o/C)}{(A_o/C)}$$

is equivalent to the above definition.

Refractive Index Measurements

Refractive index measurements were performed at 546 mμ using a Zeiss Abbe refractometer thermostated at 25°C.

Protein Determinations

Membrane "protein" was determined by the ninhydrin method (7) using crystalline bovine serum albumin and DL-serine as reference standards.

RESULTS AND DISCUSSION

I. *Turbidity of Membrane Suspensions*

A. General

The absorbance, A, and turbidity, τ, of a suspension of spherical particles are defined by the

relationships

$$A = \log I_0/I = \frac{\pi a^2}{2.3}(N)K \quad (1)$$

and

$$\tau = \ln I_0/I = \pi a^2 NK \quad (2)$$

where I_0 and I are, respectively, the intensities of the incident and transmitted light, a is the radius of the scattering particles, N is the number of particles per unit volume, and K is the scattering coefficient (i.e., the fraction of light incident on the particle that is scattered by the particle). K is a complex function of the parameters m and α, where $m = n/n_o$, the ratio of the refractive index of the scattering particles to that of the medium, and $\alpha = \frac{2\pi a}{\lambda'}$; here λ' is the wavelength of the light in the suspension medium.

Particles whose dimensions are less than $\lambda'/20$ exhibit Rayleigh scattering (8), in which case

$$K = \tfrac{8}{3}\alpha^4\left(\frac{m^2-1}{m^2+2}\right)^2 \quad (3)$$

When m approaches 1.0, *Equation 3* simplifies to

$$K = \tfrac{32}{27}\alpha^4(m-1)^2 \quad (4)$$

and one obtains for the absorbance

$$A = \frac{\pi a^2 N}{2.3} \cdot \tfrac{32}{27}\alpha^4(m-1)^2 = \frac{NV^2}{2.3} \cdot \frac{32\pi^3}{9(\lambda')^4}(m-1)^2 \quad (5)$$

and

$$\left(\frac{A}{C}\right) = \frac{4\pi a^3}{2.3\rho} \cdot \frac{32\pi^3}{9(\lambda')^4} \cdot (m-1)^2 \quad (5\,a)$$

where V is the particle volume, C the weight concentration, ρ the particle density, and $\left(\frac{A}{C}\right)$ the specific absorbance. The absorbance of a suspension of particles which are much smaller than the wavelength of light thus varies inversely as the fourth power of the wavelength of light incident in the sample.

In the case of larger particles, each portion of each particle exhibits Rayleigh scattering, but the scattering sites are in a fixed relation to each other, leading to interference between scattered wavelets (Rayleigh-Gans scattering). Moreover, in the case of slightly larger particles in which over-all dimensions are not small compared to $\lambda'/(m-1)$, phase changes producing destructive interference can take place within the particle itself. As a result, less light is scattered at angles >0, and consequently less light is extracted from the incident beam than expected from Equations 3 to 5. In such particles, the turbidity does not vary as λ^{-4} as required by Equation 5, but as λ^{-4+B}. For particles in the Rayleigh region, $B = 0$; for very large solid spheres, $B = 2$.

The problem of light scattering by spherical particles which are not small with respect to λ' has been completely solved by Mie (9). However, in the special case of spherical particles with dimensions comparable to those of the incident light and with m near 1.0, the absorbance is approximated by the Jobst equation (10):

$$A = \frac{\pi a^2}{(2.3)} \cdot N \cdot [2\alpha^2(m-1)^2] = \frac{NV6\pi^2 a_2}{(2.3)(\lambda')^2} \cdot (m-1)^2 \quad (6)$$

and

$$\left(\frac{A}{C}\right) = \frac{6\pi^2 a}{(2.3)\rho(\lambda')^2} \cdot (m-1)^2 \quad (6\,a)$$

Thus, for particles in the region of Jöbst scattering, the specific absorbance, $\left(\frac{A}{C}\right)$, is directly, proportional to the particle radius and varies inversely as $(\lambda')^2$.

B. Variation of A with λ'

We have determined the absorbance of PM and ER vesicles at wavelengths from 350 to 800 mμ.[1] The log-log plots of absorbance versus wavelength (Fig. 2) were linear and the slope of the line, $(B-4)$, was found by the method of least squares to be 2.40 $\pm$ 0.04 for three PM preparations and 2.32 $\pm$ 0.04 for three ER preparations. This is in good agreement with the calculations of

[1] Between 350 and 800 mμ absorbance is due to light scattering and not to any significant electronic band spectra.

Koch (11) which indicate that the absorbance of spherical shells would vary as the inverse 2.35 power if the increase in dn/dc between 800 and 350 mμ is taken into account.

C. Measurements of Refractive Index

The numerical computations of light-scattering functions from the Mie theory by Heller and Pangonis (12) show that for colloidal spheres with diameters ⅕ to ½ the wavelength of light, the turbidity, τ, is almost exactly proportional to $(m - 1)^2$. Therefore

$$A \propto \frac{1}{2.3} \cdot (m - 1)^2 \tag{7}$$

Accordingly, the absorbance will be zero when $m = 1.0$, i.e. when the particles are immersed in a medium of refractive index identical to their own.

However, in the case of membrane vesicles, one is dealing with spherical shells rather than solid spheres. The relative refractive index, m, of such particles in the size range under discussion can be approximated by the equation (13),

$$m = \frac{n_1}{n_o}\left(\frac{b}{a}\right)^3 + \frac{n_2}{n_o}\left[1 - \left(\frac{b}{a}\right)^3\right] \tag{8}$$

where n_1 is the refractive index of the medium within the shell, n_2 that of the shell, b the internal radius of the shell, and a the external radius.

In the case of the minute, charged, semipermeable vesicles under study, it is difficult to evaluate Equation 8 as such, since immersion of the particles in media of varying refractive index—due to varying concentrations of nonpermeant solutes—is likely to alter n_1 and $(b/a)^3$ in a quantitatively unpredictable fashion. However, in the special case in which a permeant solute is employed and the internal and external media have the same refractive index, $(n_o = n_1)$,

$$m = \left(\frac{b}{a}\right)^3 + \frac{n_2}{n_o}\left[1 - \left(\frac{b}{a}\right)^3\right] \tag{9}$$

Then, if $\left[1 - \left(\frac{b}{a}\right)^3\right] = \beta$, where β is the volume fraction of the shell,

$$(m - 1)^2 = \beta^2\left(\frac{n_2}{n_o} - 1\right)^2 \tag{10}$$

and, substituting in Equation 7

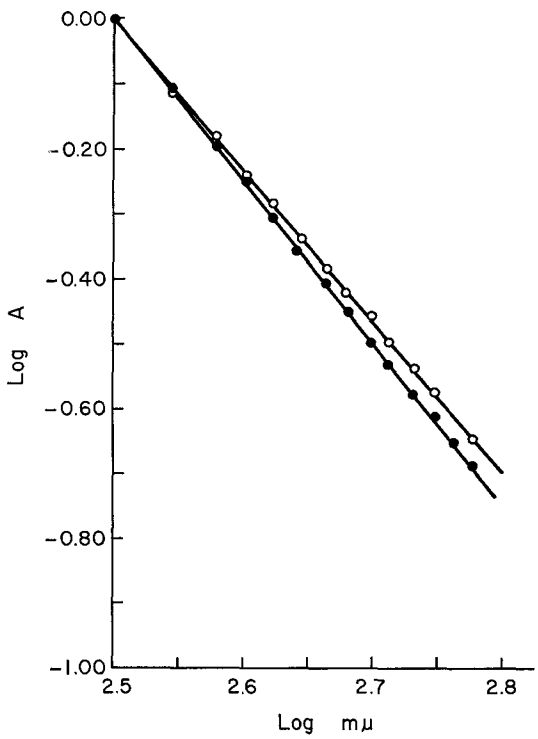

Figure 2 Variation of the absorbance of PM and ER suspensions with λ. Particle concentration, 100-μg "protein"/ml. Buffer, 0.001 M Tris-HCl (pH 8.2). For clarity of comparison, Log A was set to zero at Log mμ 2.5. PM, ●——●; ER, ○——○.

$$A \propto \frac{\beta^2}{2.3}\left(\frac{n_2}{n_o} - 1\right)^2 \tag{11}$$

i.e. a plot of $(A)^{1/2}$ against $1/n_0$ will give a straight line intercepting the abscissa when $n_0 = n_2$, with a slope determined, among other factors, by the value of β.

We have employed glycerol-water mixtures for the evaluation of n_2. Glycerol was chosen because it can penetrate into the vesicles (14, 15), because it does not appear to injure the ATPase, diaphorase, and antibody-binding properties of the membranes, and because fairly high refractive indices can be obtained with it.

The particles were suspended in appropriately buffered glycerol-water mixtures, mixed thoroughly, and the absorbances and refractive indices measured at 546 mμ and 25°C after 5 and 17 hr storage at 4°C. Before each optical measurement the suspensions were mixed again and then briefly centrifuged at 1000 RPM to remove air bubbles.

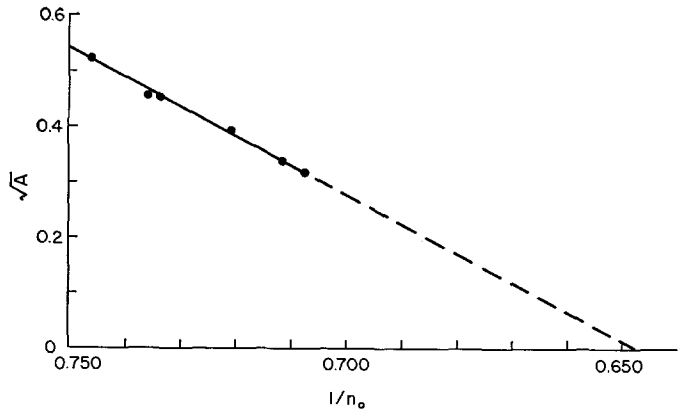

FIGURE 3 Variation of the absorbance of PM suspensions with the refractive index, n_o, of the suspension medium (glycerol-water mixtures). Extrapolation of A to O locates the point at which the refractive index of the medium is equal to that of the vesicle wall. Measurements were at 546 mμ. See text for details.

Plots of $(A)^{1/2}$ against $1/n_o$ (Fig. 3) were linear. The values of n_2 obtained from such graphs (fitted by aid of an IBM 1620 computer) were 1.553 ± 0.006 (SD) for three preparations of PM in 0.001 M Tris-HCl, pH 8.2. The values obtained for different preparations of ER were more variable and ranged between 1.549 and 1.601. The values of n_2 at pH 2 to 4.3 did not differ measurably from those obtained at pH 8.2.

Because of the long extrapolations required, the evaluation of n_2 lacks the precision to detect subtle refractive index differences such as might exist between ER and PM and which might accompany pH or other environmental alterations. Moreover, this extrapolation procedure is strictly justifiable only if all vesicles in the population have the same wall refractive index n_2. Otherwise, some of the particles will be scattering light for whatever value of n_o is chosen, and extrapolation should be made to some small absorbance value greater than zero. In this case, that n_o which gave a minimum absorbance would correspond to the most prevalent value of n_2 for the population. This assumption that the population is homogeneous in respect to n_2 is not unlikely. Our values for the refractive indices of PM and ER are consistent with those found for lipid bilayer membranes (1.66) by Brewster angle determinations (16). The large values are most likely due to the tight packing of lipids in these membranes.

We have obtained an approximate value for the relative refractive index, m, in 0.001 M Tris-HCl (ph 8.2) by means of Equation 8 as follows:

n_2 was determined as described above; n_1 was taken to be equal to n_o = 1.334, the refractive index of 0.001 M Tris-HCl, since the vesicles had been osmotically "shocked" in this medium during preparation (5, 6).

β was evaluated from the relationship (15):

$$\rho_p = (1 - \beta)\rho_f + \beta\rho_w \qquad (12)$$

where ρ_p, the density of the whole spherical vesicle, is the sum of the volume-weighted densities of the hydrated wall, ρ_w, and of the internal fluid, ρ_f, (0.997 in the present case).

ρ_p, determined by ultracentrifugal equilibration of PM in Ficoll density gradients buffered with 0.001 M Tris-HCl to pH 8.2, was found to be 1.045 at 25°C (5). ρ_w, measured by equilibration in similarly buffered glycerol gradients, was found to have a median value of 1.150 (15).

From these data, β, the volume fraction of the hydrated membrane wall of PM vesicles, calculates to be 0.314 under the cited conditions. Equation 10 then gives a relative refractive index of 1.050.

D. Estimation of Average Particle Size and Particle Number in PM Suspensions

1. PARTICLE SIZE: We have estimated the average vesicle radius as follows:

The A_{546} of a suspension of PM in 0.001 M

Tris-HCl (pH 8.2), containing 1 mg of membrane "protein" per ml, is 0.775 ± 0.002. This quantity of vesicles, whose density is 1.045 at 25°C, occupies a volume of 6.21 ± 0.31 mm^3, i.e. the total wet mass associated with 1 mg of PM "protein" is 6.5 mg. Consequently, the A_{543} of a PM suspension containing 1 mg of *hydrated* vesicles per ml is 0.120. According to the tabulations of specific turbidities computed from the Mie theory for $\lambda = 546$ mμ and $m = 1.05$ (12), this specific absorbance corresponds to an average particle radius of *717 A*.

If 717 A is the average value of a, the external radius of the membrane shell, the internal radius, b, computed from the relationship $\beta = \left[1 - \left(\frac{b}{a}\right)^3\right] = 0.314$ (vide supra), comes out to be *632 A*, giving a membrane thickness of *85 A*. This value is in good accord with other estimates of the thickness of cellular membranes. Moreover, the particle dimensions computed above are consistent with an average diameter of 1500 A found electronmicroscopically (17).

Data on ER vesicles are less complete, but suggest that their dimensions are similar to those of PM vesicles when 0.001 M Tris-HCl (pH 8.2) is the suspension medium.

2. PARTICLE NUMBER: We have calculated an estimate of the average number of PM vesicles corresponding to 1 mg protein as follows:

From the dimensions listed above, the areas of the outside and inside surfaces of a typical vesicle together add up to about 1.2×10^7 A^2/vesicle. However, the lipids associated with 1 mg of PM protein can cover an area of about 2.4×10^{19} A^2 as a monolayer, assuming an area of 50 A^2/molecule (18). Consequently, one mg of PM protein corresponds to about 2×10^{12} *vesicles*.

II. *Effects of Changes of Ionic Environment upon the Turbidities of Membrane Suspensions*

A. Stability of Particulate Suspensions—Theoretical Considerations

1. GENERAL: The number, C, of collisions per second between particles in a suspension is given by the relationship (19)

$$C = \frac{4kTN^2}{3\eta} \tag{13}$$

where kT is the thermal energy unit (4.14×10^{-14} $g \cdot cm^2 \cdot sec^{-2}$ at 25°C), N is the number of particles per cm^3 and η is the viscosity (0.01 $g \cdot cm^{-1} \cdot sec^{-1}$ for water at 25°C). For aqueous suspensions containing about 2×10^{11} particles per cm^3, the collision rate is about 2×10^{11} encounters per sec.

Whether or not such encounters lead to particle adhesion depends upon the attractive and repulsive forces acting between particle surfaces and between the particles and water (20). Possible attractive forces include: (1) ion-pair and ion-triplet formation; (2) forces due to charge fluctuations (21); (3) electrostatic attractions between charge mosaics on surfaces of like (or opposite) net charge; (4) electrostatic attractions between surfaces of like charge but different potential (22); (5) electrostatic attraction due to "image forces" (23); (6) diminution of free energy due to decrease with aggregation of the interfacial area between particles and solvent; (7) Van der Waals forces.

Two factors act in opposition to the above forces and tend to make particle collisions elastic and reversible. These are: (*a*) electrostatic repulsion between surfaces of like charge and (*b*) hindrance to attractive forces by layers of structured water on the particle surfaces.

The rate of decrease in the number of particles per cm^3 is

$$-dN/dt = \frac{4kTN^2}{3\eta} \cdot e^{-(W_R/kT)} \tag{14}$$

for spherical particles. Here W_R is the net energy barrier to aggregation.

The time, $t_{1/2}$, for the particle number to be reduced to ½ of the initial value, N_o, is then:

$$t_{1/2} = (3\eta/4kTN_o)e^{W_R/kT} \tag{15}$$

For aqueous dispersions at 25°C this becomes

$$t_{1/2} = (2 \times 10^{11}/N_o)e^{W_R/kT} \tag{16}$$

Equations 14 to 16 are approximate only, since they assume that attractive forces do not operate until particle contact and also that there is no redispersion.

A major factor in the stability of membrane suspensions is the electrostatic repulsive energy, W_E, between particles of like charge due to the ionic double layer associated with ionogenic groups fixed on the particle surfaces. It is approximately (19):

TABLE I

Particle conc.	Conditions for							
	t ½ = 0.5 hr				t ½ = 24 hr			
	ψ_0 (mv)	W_R (kT)	Γ/2 at Area/Charge ($A^2 \times 10^{-3}$) 1.8	2.7	ψ_0 (mv)	W_R (kT)	Γ/2 at Area/Charge ($A^2 \times 10^{-3}$) 1.8	2.7
2×10^{10}	−10.0	5.2	0.152	0.068	−13.1	9.0	0.089	0.038
2×10^{11}	−12.0	7.5	0.102	0.046	−14.8	11.4	0.068	0.030
2×10^{12}	−13.7	9.8	0.080	0.035	−16.2	13.7	0.057	0.025
2×10^{13}	−15.2	12.1	0.064	0.029	−17.5	16.0	0.046	0.021
2×10^{14}	−16.6	14.4	0.054	0.024	−18.7	18.3	0.044	0.019

Calculations are made to estimate that ionic strength which will result in aggregation half-times of ½ hr and 24 hr for various particle concentrations. We assume that there is no ion-binding or long range attractive forces, and that only univalent electrolytes are present. Calculations are for particles of 700-A radius at neutral pH, and are given both for particles with an area/charge of 1.8×10^3 A^2/charge and for particles with a lower charge density (2.7×10^3 A^2/charge), as is found on liver mitchondria (24).

$$W_E = \frac{D\psi_0^2 a}{2} \cdot \ln (1 + e^{-\kappa d}) \qquad (17)$$

where D is the dielectric constant, ψ_0 is the surface potential in millivolts, a is the particle radius in *cm*, d is the distance between their nearest points in *cm*, and $1/\kappa$ is the thickness of the double layer in *cm*. At contact, where $d = 2a$,

$$W_E = 0.35\, D\psi_0^2 a \qquad (18)$$

The value of the potential, ψ_o, at the plane of the ionic groups is given by the Gouy equation (19):

$$\psi_0 = \frac{2kT}{e} \operatorname{Sinh}^{-1}\left(\frac{134}{AC_i^{1/2}}\right) \qquad (19)$$

where e is the protonic charge (4.77×10^{-10} esu., $2kT/e = 52$ *mv* at 25°C. A is the area in $(A)^2$ per fixed ionic group, and C_i is the concentration of uni-univalent electrolyte in the bulk phase in moles/L.

The above considerations can be used to evaluate the theoretical stability of suspensions of PM vesicles. Thus, the area per fixed anionic group on the PM of intact EAC has been found by electrophoretic means to be at most 1.8×10^3 A^2 near neutrality (1). From this, one can compute approximate values of ψ_o for various ionic strengths from the Gouy equation. The theoretical aggregation rates can then be evaluated by use of Equations 18 and 16. The results of such calculations are given in Table I.

The calculations show that, within the specified limitations, even the highly concentrated particle suspensions encountered in cell fractionation procedures (2×10^{14} particles/cm^3 is about equivalent to a 30% (v/v) suspension) are unlikely to aggregate provided the Γ/2 is kept below about 0.02. Moreover, at the particle concentrations used for the assay of ion-sensitive ATPases ($2–4 \times 10^{10}$ particles/cm^3), aggregation is relatively slow even at the high Γ/2 used in these assays (3). It should be noted, however, that the above stability calculations are only rough estimates because of the quantitatively unknown role of hydration and steric barriers to adhesion and because of the possible operation of long range attractions.

In any event, at higher Γ/2 aggregation may become appreciable even at neutral pH. Moreover, reduction of the charge by removal or titration of ionogenic groups or by binding of counterions will lower ψ_o and may lead to rapid aggregation even at low particle concentrations.

2. EFFECT OF AGGREGATION ON TURBIDITY: When aggregation occurs it will lead to changes in turbidity due to alterations in the number, size, and geometry of the scattering particles. We have shown that the radius of PM vesicles is approximately 717 A and that the effective refractive index of such vesicles is roughly 1.05. The specific absorbance of such particles (and small clusters thereof) is, therefore, adequately described by the Jöbst approximation (Equation 6 *a*). That this is so is clear from the computations of Heller and Pangonis (12) which

show that, when $\lambda' = 3000$ A, the specific absorbance varies in direct proportion to the particle radius, a, between $a = 500$ A and $a = 3000$ A for $m = 1.05$, (and between $a = 500$ A and $a = 2500$ A for $m = 1.10$). So we shall present an expression for the rate of change of absorbance, dA/dt, for aggregation of particles in the Jöbst region together with a calculation of the fractional absorbance increment, Δ, for particles in this region.

a. *Rate of change of absorbance, dA/dt.* The rate of change of absorbance for aggregating Jöbst particles is:

$$dA/dt = \frac{4kT}{(2.3)3\eta} \cdot e^{-(W_R/kT)} N_o \left(\frac{C}{\rho}\right) \frac{6\pi^2 a_o}{(\lambda')^2} (m-1)^2 \quad (20)$$

This rate varies linearly with a_o, the radius of the primary particle.

Calculations using the equations of Oster (25), which describe the rate of change of absorbance for particles in the region of Rayleigh scattering, show that a suspension of particles exhibiting Jöbst scattering would be expected to have a $\left(\frac{dA}{dt}\right)$ roughly 1.5 times that of a suspension with Rayleigh scattering, assuming identical values of C, ρ, T, η, W_R, and λ in the two systems.

No simple equation exists for the dA/dt of a suspension of particles with radius >3500 A ($m = 1.05$). This is because the scattering coefficient, K, oscillates as a gets large.

b. *Fractional absorbance increment.* We derive the maximum Δ attributable to the aggregation of Jöbst particles as follows:

1) Assume that all aggregates (hereafter termed *i-mers* for aggregates containing i original vesicles) as well as the original vesicles are spherical. (Any other geometry will give lesser Δ's.)

2) Assume that the volume of the *i-mer* formed is equal to that of the vesicles of which it is composed. This implies that

$$a_{i\text{-}mer} = a_o \sqrt[3]{i} \quad (21)$$

where $a_{i\text{-}mer}$ = radius of the *i-mer* and $a_o = 717$ A, the average radius of the primary particle.

Now, applying Equation 6 to each i-mer and summing on all i-mers to find the total absorbance after aggregation, we obtain A, the total absorbance after aggregation:

$$A = \sum_{i=1}^{\text{maximum i-mer}} (N_i V_i a_{\text{i-mer}}) \frac{6\pi^2(m-1)^2}{2.3(\lambda')^2} \quad (22)$$

where N_i is the number concentration of i-mers and V_i and a_i are, respectively, the volume and radius of the i-mer.

Before aggregation the absorbance, A_o, is:

$$A_o = N_o V_o a_o \frac{6\pi^2(m-1)^2}{2.3(\lambda')^2} \quad (23)$$

where N_o is the original number of vesicles and V_o and a_o are the volume and radius, respectively, of the original vesicles.

Defining $f_i = iN_i/N_o$ = weight fraction of i-mers, we can write

$$\frac{A}{A_o} = \sum_{i=1}^{\text{maximum i-mer}} \left(\frac{N_i}{N_o}\right)\left(\frac{V_i}{V_o}\right)\left(\frac{a_i}{a_o}\right) = \sum_{i=1}^{\text{maximum i-mer}} \left(\frac{f_i}{i}\right)\left(\frac{V_i}{V_o}\right)\left(\frac{a_i}{a_o}\right) \quad (24)$$

But, since $V_i/V_o = i$ and $a_i/a_o = \sqrt[3]{i}$,

$$\frac{A}{A_o} = \sum_{i=1}^{\text{maximum i-mer}} (f_i)(\sqrt[3]{i}) \quad (25)$$

Therefore,

$$\Delta = \frac{A - A_o}{A_o} = \left(\sum_{i=1}^{\text{maximum i-mer}} (f_i)(\sqrt[3]{i})\right) - 1 \quad (26)$$

or

$$\Delta + 1 = \sum_{i=1}^{\text{maximum i-mer}} (f_i)(\sqrt[3]{i}) \quad (27)$$

Hence, if f_i, the weight distribution of i-mers, is known, Δ can be estimated quantitatively. We shall discuss this point further in examining experimental data.[2]

[2] An exactly analogous derivation for particles in the region of Rayleigh scattering shows that

$$\Delta + 1 = \sum_{i=1}^{\text{maximum } i\text{-mer}} (f_i)(i)$$

But the approach is not applicable to very large particles in which absorbance is not a simple function of radius.

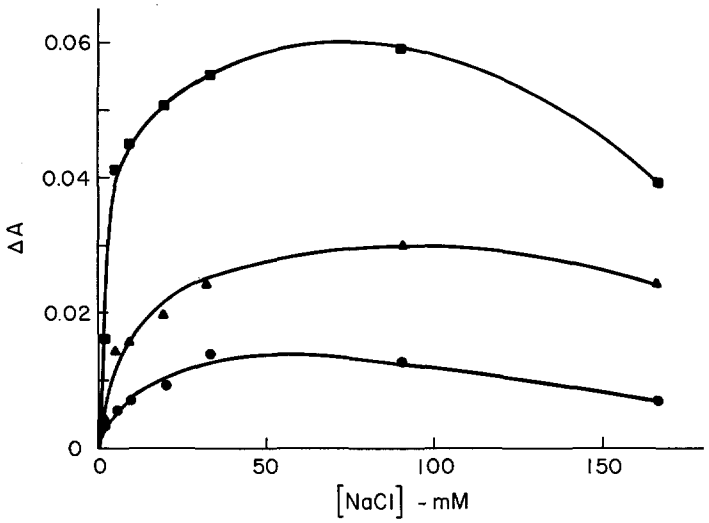

FIGURE 4 Effect of sodium chloride on the absorbance of membrane vesicles. λ is 400 mμ. ΔA is the absolute increase in absorbance "per cm optical path" for suspensions containing 100 g protein per ml. Buffer, 0.001 M Tris-HCl (pH 8.2). PM, ●——●; 1.025 component, ▲——▲; ER, ■——■.

B. Specific Alterations of the Turbidity of Membrane Suspensions

1. EFFECTS OF UNIVALENT ELECTROLYTES: The effect of increasing concentrations of NaCl upon light scattering by various membrane fragments is illustrated in Fig. 4. The experiments were performed using 0.001 M Tris-HCl to buffer to a measured pH of 8.20 ± 0.05. After measurement of the absorbance in this medium, appropriate amounts of 1 M NaCl were added and the absorbance measured 30 and 60 sec after mixing and then at 60-sec intervals.

Addition of NaCl increases light scattering by all three vesicle types. At a particle concentration of 100 to 500 μg protein/ml, more than 90% of the fractional absorbance increment seen 5 min after mixing occurs within 30 sec. Absorbance is maximal in the range of 50 to 100 mM NaCl and diminishes at higher salt levels. Similar effects are obtained with KCl and NaBr.

The greatest change occurs with suspensions of ER vesicles, which give a maximum fractional absorbance increment $\Delta = 0.50$ compared with $\Delta = 0.08$ for PM and $\Delta = 0.07$ for the $\rho = 1.025$ component. Moreover, the fractional absorbance increment of ER suspensions does not diminish significantly when the particle concentration is lowered from 100 to 10 μg per ml—by use of cuvettes with a 10-cm light path—whereas the salt effect disappears with a similar reduction in the concentration of PM vesicles (vide infra).

2. EFFECTS OF CALCIUM AND MAGNESIUM: Addition of $CaCl_2$ or $MgCl_2$ to suspensions of the various membrane vesicles in 0.001 M Tris-HCl (pH 8.2) produces striking increases in absorbance (Fig. 5 *a* and *b*). These are much larger than the changes obtained with NaCl, particularly in the case of ER. Also, the light-scattering changes effected by Ca^{2+} and Mg^{2+} occur at much lower ionic concentrations. At a given concentration between 0 and 15 mM, Ca^{2+} raises absorbance more than Mg^{2+}. At particle concentrations between 6 and 600 μg protein/ml, more than 70% of the fractional absorbance increment at 5 min occurred within 30 sec after the addition of Ca^{2+} or Mg^{2+}. A continued increase in absorbance, diminishing in rate with time, was observed at concentrations greater than 200 μg/ml.

a. *PM vesicles.* Addition of Ca^{2+} or Mg^{2+} to suspensions of PM produces a fractional absorbance increment of $\Delta = 0.21$ and 0.08, respectively, for measurements taken 5 min after addition of divalent cations to a concentration of 15 mM (at a protein concentration of 100 μg/ml). Are there any likely weight distribution functions, f_i, which can account for these values of Δ? We consider first the simple case of complete dimerization in

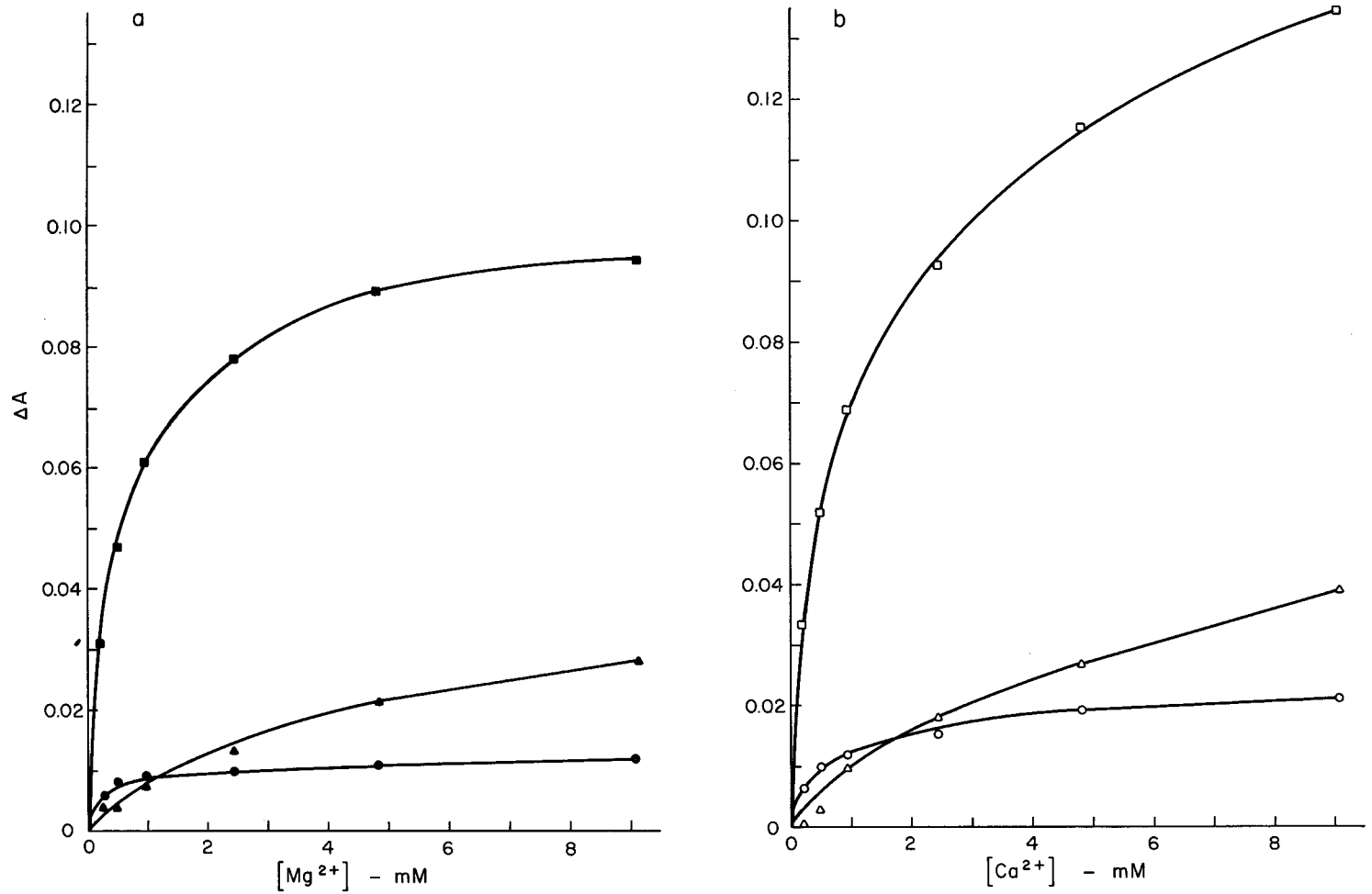

FIGURE 5 Effect of Mg^{2+} and Ca^{2+} on the absorbance at 400 mμ of membrane suspensions in 0.001 M Tris-HCl (pH 8.2). ΔA is the absolute increase in absorbance "per cm optical path" for suspensions containing 100-μg protein/ml. Fig. 5 *a*, effects of Mg^{2+}. PM, ●——●; ρ 1.025 component, ▲——▲; ER, ■——■. Fig. 5 *b*, effects of Ca^{2+}. PM, ○------○; 1.025 component, △——△; ER, □——□. Time of observation, 5 min after mixing.

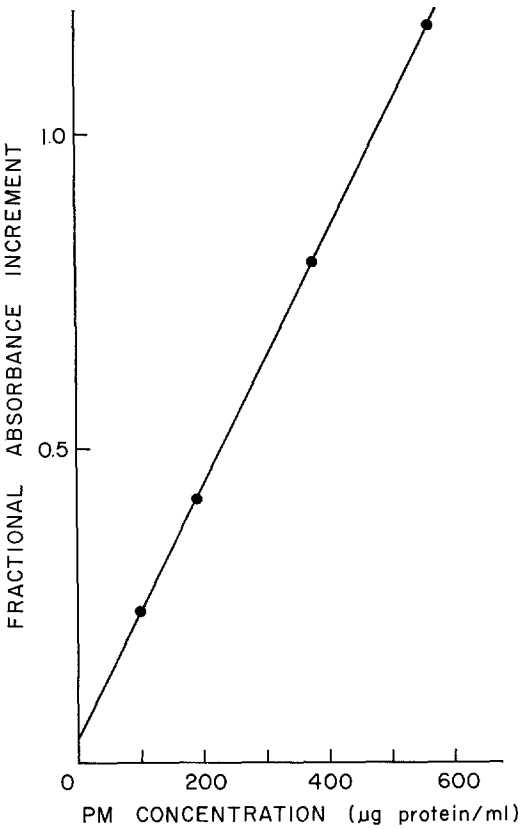

FIGURE 6 Effect of Ca^{++} addition (to 15 mM) upon PM suspensions of varying particle concentration. Buffer, 0.001 M Tris-HCl (pH 8.2). Time of observation, 5 min after mixing. λ is 400 mμ.

which all the particles aggregate to form only dimers. Then $i = 2$, f_2 (the weight fraction of dimers) = 1, and $f_i = 0$ for $i \neq 2$. Then from Equation 27 $(1 + \Delta) = 1.26$ and $\Delta = 0.26$.

Thus, mere dimerization could account reasonably well for the $\Delta = 0.21$ observed upon Ca^{2+} addition. A similar calculation reveals that a mixture of monomers ($f_1 = 0.69$) and dimers ($f_2 = 0.31$) would have a $\Delta = 0.08$. Therefore, partial dimerization could account fully for the Δ observed upon addition of Ca^{2+} or Mg^{2+}.

Of course, there is no good reason to assume that aggregation ceases after dimerization (i.e. that $f_i = 0$ for $i > 2$). Indeed, the appearance of particles which are readily sedimented at low gravitational force and which are visible in the light microscope is strong evidence that some higher aggregates are formed.

We now examine the behavior of PM suspensions of varying protein concentration, and find from Fig. 6 that $\Delta = 2.0 \times 10^{-3} C + 0.04$, where C is measured in μg protein/ml. The fact that Δ gets very small as C tends to zero supports the hypothesis that the fractional absorbance increment can in this case be attributed entirely to aggregation.

However, although flocculation can fully account for the turbidity changes produced by addition of Ca^{2+} or Mg^{2+} to PM suspensions, the rapidity with which aggregation occurs requires special comment. Thus, at a PM concentration of 100 μg/ml (2×10^{11} particles/ml), aggregation appears complete within 30 sec after raising $[M^{2+}]$ from 0 to 5 mM, although with an equivalent $\Gamma/2$ of uni-univalent electrolyte, ψ_o would be about 100 mv which would give very high stability. The speed of aggregation in the presence of Ca^{2+} or Mg^{2+} is most likely due to specific binding of these ions to the surfaces of PM vesicles. Then ψ_o is less than calculated from the Gouy equations at equivalent $\Gamma/2$ (19), and the stability of negatively charged disperse systems varies approximately as the inverse 6th power of the valence, with Ca^{2+} reducing stability somewhat more than Mg^{2+} (26).

The above explanation does not exclude the additional operation of long range electrostatic attractions. Indeed, the rapid aggregation of PM at moderate, but not high concentrations of NaCl may be due to attractions such as image forces (23), which diminish at high $\Gamma/2$ because of electrostatic screening.

b. *ER vesicles.* There is no doubt that the absorbance changes obtained with ER are in part due to aggregation. This can be shown microscopically and centrifugally and is presumably the cause of the small, concentration-dependent increase of absorbance with time. However, unlike PM, the fractional absorbance increment of ER is largely independent of concentration and remains within the range of $\Delta = 0.93 \pm 0.06$ at $t = 0$, ($\Delta = 0.99 \pm 0.11$ at $t = 5$ min), over the 100-fold range of particle concentrations examined.

These findings must be considered in the light of the observation (4, 5) that addition of Ca^{2+} or Mg^{2+} produces a large increment in the density of ER vesicles, while affecting PM vesicles to a much smaller degree. This is the basis for the separation of the two membrane types. The density change is due to loss of water from the vesicle interior, which can be explained on the

basis of decreasing Donnan effect (15). Such extrusion of water would raise the relative refractive index, m (as is apparent from Equations 9 to 12), and thus increase the absorbance of spherical vesicles (Equation 6), since this varies as the square of $(m - 1)$, but only directly as ρ^{-1} or a. We, therefore, believe that the turbidity increment produced by the addition of salts to ER suspensions represents primarily a "structural" change in these membranes. However, it must be emphasized that lack of turbidity change does not exclude a change in m since this may be counterbalanced by alterations of vesicle volume and shape. Unfortunately, we cannot, at present, evaluate small changes in m independently because of uncertainty as to the precise effects of ionic changes on vesicle geometry.

c. $P = 1.025$ *vesicles.* These particles behave like

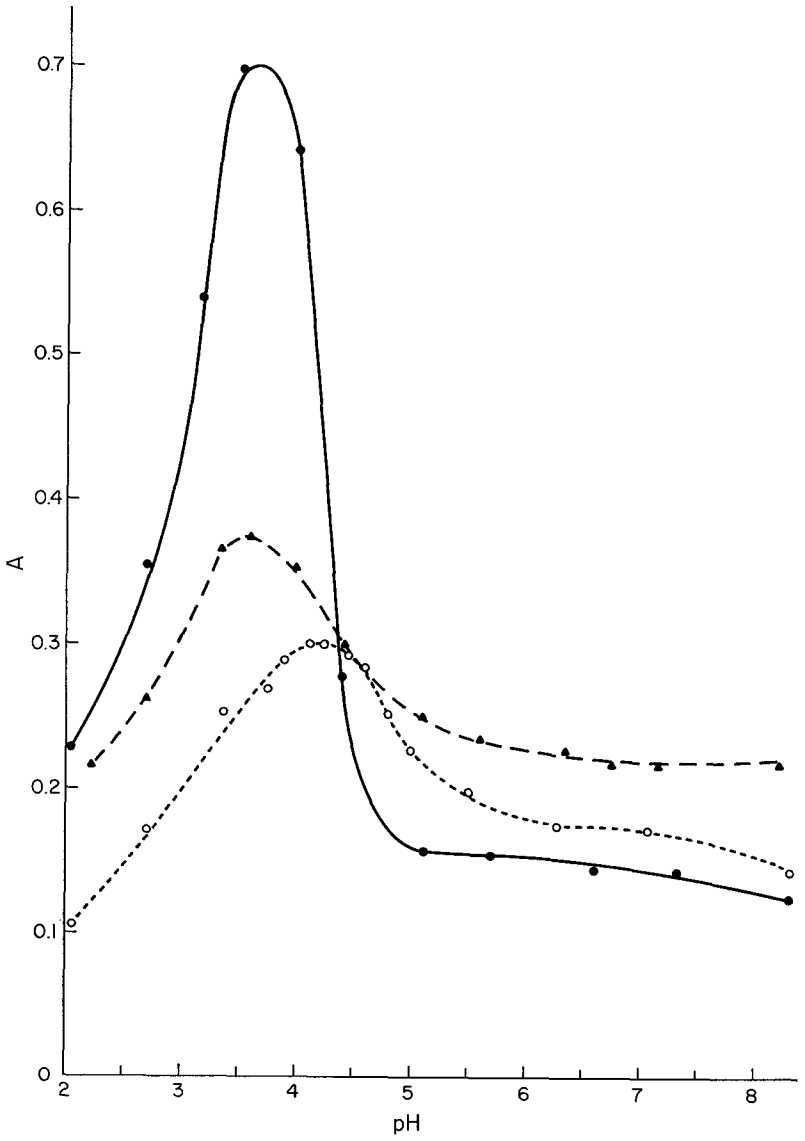

FIGURE 7 Absorbance of three types of membrane particles at different pH levels. Particle concentration, 100-ug protein/ml. Absorbances were recorded 30 min after reduction of pH from 8.2. PM, ●——●; ρ 1.025 component, ▲- - - - -▲; ER, ○- - - - -○. λ is 400 mμ.

PM, at low salt concentrations, but exhibit a fractional absorbance increment which varies linearly with $[Ca^{2+}]$ or $[Mg^{2+}]$ in the range examined.

3. VARIATION OF THE TURBIDITY OF MEMBRANE SUSPENSION WITH PH: The effect of pH upon the turbidity of membrane suspensions was measured as follows:

The membrane particles were prepared, as described before, and suspended in 0.001 M Tris-HCl (pH 8.2) to a concentration of 1 to 2 mg protein/ml. Representative samples (0.025 to 0.25 ml) were then injected into 3 ml (for 1-cm cuvettes) or 30 ml (for 10-cm cuvettes) of buffers of desired composition contained in 10- or 50-ml beakers. The suspensions were stirred vigorously for 15 sec and the pH determined using an Instrumentation Laboratories Model 135A pH meter with an Ingold Model 14040 combination electrode (Instrumentations Laboratory Inc., Watertown, Massachusetts). The suspension was then transferred to an appropriate cuvette and the absorbance read against a buffer blank beginning 30 sec after initiation of mixing and at 30- and 60-sec intervals thereafter (unless stated otherwise). The pH was again measured after termination of absorbance measurements and was always within 0.03 pH units of the initial measurement. Tris-acetate buffers were used except for pH levels of 3 and less which were attained by addition of dilute HCl to the buffer system. The ionic strength was 0.01 unless stated otherwise. The comparative variation of absorbance of the three membrane types under discussion is illustrated in Fig. 7.

Measurement of the variation of turbidity with pH by continuous titration of membrane suspensions with acid or base was unsatisfactory because of the increase of absorbance with time during aggregation induced by pH changes.

a. *PM vesicles.* i) *pH-turbidity profile:* The pH-turbidity relation is given in Fig. 8 *a* for a con-

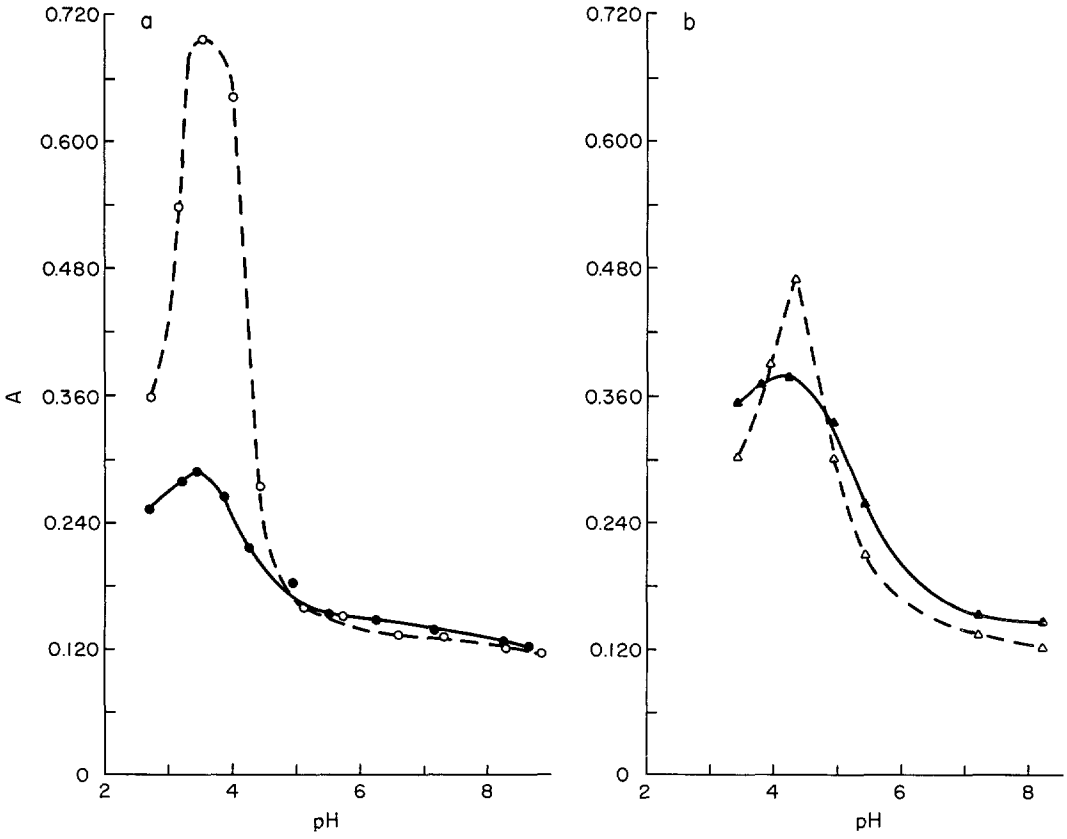

FIGURE 8 Absorbance of PM and ER at varying levels of pH and at two salt concentrations. Fig. 8 *a*, (Left panel) PM; $\Gamma/2 = 0.01$; ○------○; $\Gamma/2 = 0.11$; ●——●. Fig. 8 *b*, (Right panel) ER; $\Gamma/2 = 0.01$; △------△; $\Gamma/2 = 0.11$; ▲——▲. λ is 400 mμ.

centration of 100 μg protein/ml and for Γ/2 = 0.01 and 0.11. The absorbance changes only slightly as pH is lowered from above 8 to 5.0, then rises sharply, reaching a maximum at pH 3.60 ± 0.15 and declining abruptly thereafter. The absorbance at pH 2 is about the same as at pH 8. Above pH 4.5 and below pH 3.0 the absorbance change is essentially complete 60 sec after mixing, but between pH 4.5 and 3.0 the absorbance continues to rise after the initial increment at a rate which declines with time. Stable absorbance values are obtained by 30 min. Both the initial and the slow absorbance changes are greatest at pH 3.6 and at low Γ/2. Under these last conditions, the absorbance 1 min after mixing is only about 20% of the value measured after 30 min.

Return to pH 8.2 30 min after the initial pH change leads to a decrease in absorbance toward the control value. However, in the case of particles exposed to pH 3.2 to 4.2, the absorbance is still twice that of control even 15 hr after return to pH 8.2.

ii) *Effect of particle concentration:* In order to establish the role of aggregation in the turbidity changes initiated by pH variation we have measured the fractional absorbance increment obtained with different particle concentrations at various time intervals after reduction of pH from 8.2 to 3.6 at Γ/2 = 0.01.

The small fractional absorbance increment Δ = 0.32 ± 0.06 (obtained at PM concentrations between 0.7 and 14 μg/protein per ml) is considered to have a structural basis since it is invariant with concentration and time.

At higher particle concentrations, the absorbance continues to rise for about 20 min at a rate increasing with particle number, but diminishing with time. At PM concentrations of 50 μg/ml or more the absorbance increment after 60 sec is less than 10% of the Δ after 30 min. We, therefore, conclude that at the higher particle concentrations more than 90% of the Δ is attributable to aggregation and that the pH-turbidity profiles strongly reflect interactions *between* particles.

Our data show that PM surfaces bear a net negative charge above pH 3.6—the apparent isoelectric point—and a net positive charge below. In both regions of charge excess, the vesicles are well stabilized against aggregation. It should also be noted that turbidity changes are small above pH 5.0 at both Γ/2 = 0.01 and 0.11, although particle stability is very sensitive to

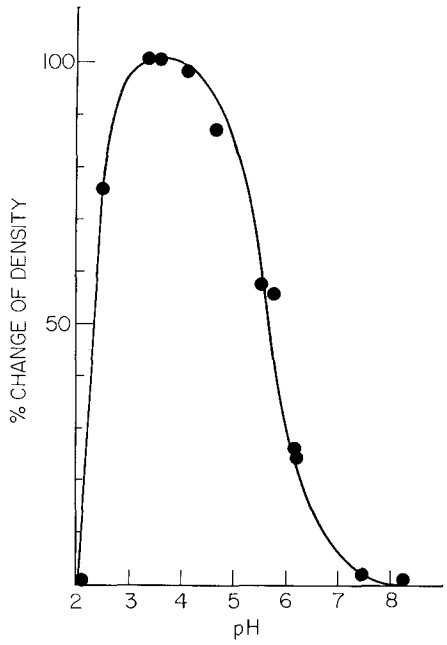

FIGURE 9 Variation in the total density of PM vesicles with pH. See text for details.

reduction of charge density at the higher ionic concentration (Equation 19). This suggests that the bulk of the anionic groups on PM surfaces have pKs ≈ 5.0. The value of 3.6 for the "isoelectric" point is in good accord with electrophoretic data which indicate that the surfaces of intact EAC bear zero net charge at pH 3.6 ± 0.5 (27–30).

Evaluation of the meaning of the small, "structurally based" changes of PM turbidity with pH is aided by analysis of the pH-density relationships of these vesicles. Fig. 9 illustrates the variation of the *total* density of PM with pH, as determined by ultracentrifugal equilibration in Ficoll gradients at Γ/2 = 0.01 and stated pH. The maximum total density, 1.09, occurs at pH 3.6 but the density of the hydrated vesicle *walls* (measured in glycerol gradients) is approximately the same, (1.15), at the isoelectric point as at pH 8.2.[3] The increase in *total* density from 1.045 at pH 8.2 to 1.09 at pH 3.6 must, therefore, be due principally to extrusion of water from the vesicle interior rather than from hydration layers (15).

Although the pH range of maximum total density coincides with the isoelectric region deter-

[3] The density of the hydrated PM wall is greatest (1.175) at about pH 5.

mined turbidimetrically, a major increment in *total* density occurs between pH 6.5 and 4.5, where aggregation-induced absorbance changes are small. Since aggregation depends upon the state of dissociation of anionic groups on *external* PM surfaces, we relate the density increment between pH 6.5 and 4.5 to the titration of groups fixed on internal surfaces or within the membrane structure. Titration of anionic sites on the external surfaces may add to the density increment below pH 5.0. The density and absorbance decrements below pH 3.6 are attributable to increasing positive charge excess on both external and internal sites.

The relatively large increase in density between pH 8.2 and 3.6 implies an increase in β, the volume fraction of the vesicle wall. One might, therefore, infer that the relative refractive index would necessarily increase (Equations 8 to 10) leading to a large, positive Δ. The fact is, however, that the Δ observed prior to aggregation is only $+0.3$. This relatively small value of Δ seems at first inconsistent with the large increase in density. However, the discrepancy is only apparent.

There are two fundamental geometrical transformations which will raise β sufficiently to produce the observed increases in density, namely: (*a*) deformation of the spherical vesicles into less symmetric structures, and (*b*) fragmentation of the original particles into a larger number of smaller vesicles.

In the case of deformation, one can imagine transformations of the spheres into equivalent right circular cylinders of the same wall volume. Such cylinders, having the observed density of 1.09, would be 332 A tall and would have an outer radius of 875 A and a wall thickness of 85 A. β for these cylinders would be 0.60 (vs. 0.31 for the original spheres), and, on the basis of the volume-weighting approximation (Equation 10), the relative refractive index, m, would rise from 1.05 to about 1.10. The absorbance prior to aggregation should then be more than three times higher at pH 3.6 than at pH 8.2 (i.e. $\Delta = 3.00$), even after the effects of altered density and geometry on Equation 6 are taken into account. This is clearly not in accord with the observed Δ of about 0.3.

On the other hand, the density increment between pH 8.2 and 3.6 can also come about through a fragmentation of the vesicles into small spheres of mean radius 320 A and of 85-A wall thickness. This transformation would raise the volume fraction of the wall to about 0.60 and the relative refractive index to about 1.10. However, because of the great reduction in particle volume, the specific absorbance would now *decrease* by about 25%. Of course, these smaller particles would probably aggregate very rapidly (because of the decrease in W_E with diminishing particle radius Equations 17 and 18), possibly leading to a Δ of >0.

Thus, the observed $\Delta = +0.3$ may be explained entirely on the basis of fragmentation into small vesicles and subsequent aggregation. A combination of deformation of some vesicles, leading to a net increase in Δ, together with some fragmentation of vesicles (with or without aggregation), leading to a net decrease in Δ, could also account for the observed $\Delta = 0.3$. This combination of fragmentation and deformation is consistent with electron micrographs of membranes fixed at isoelectric pH, which show deformed profiles of reduced dimensions and, in some cases, even apposition of internal surfaces, while the outlines are circular in the case of membranes fixed at pH 8.2 (17).

Thus, reasonable geometric transformations can account for both the marked increase in density and the slight rise in the structurally based Δ. There is no necessary inconsistency. However, one should consider two other possible explanations of this apparent discrepancy. First, because the high refractive index of the vesicle wall is largely due to the tightly packed membrane lipid, a change in phase of this component from a continuous bilayer to an array of small micelles within the membrane (31) would be expected to reduce absorbance substantially. A small degree of phase change combined with the deformation transformation could thus yield the net, small, positive Δ observed. Secondly, we note that the measurements of Δ were made within minutes (and extrapolated to time zero). We have tacitly assumed that the measurements of density, which require many hours, accurately reflect the density at the times at which Δ was determined. We consider this a good assumption (in view of the kinetics of mitochondrial volume changes), but it is possible that deformation, for example, is a slow process. A small degree of deformation would then be reflected in a small positive Δ in the first 30 min, while, hours later, when the deformation is complete, it would give a large density increment.

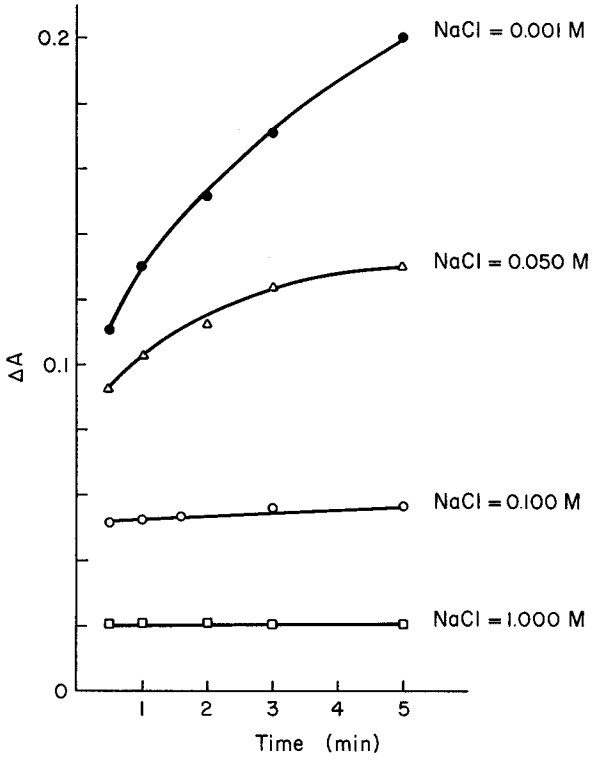

FIGURE 10 The effect of salt concentration upon the extent and rate of absorbance change of PM initiated by reduction of pH from 8.2 to 3.6. Particle concentration is 100 μg protein/ml. ΔA is the change in total absorbance "per cm optical path" at 400 mμ at varying time intervals after pH reduction.

iii) *Effect of* $\Gamma/2$ *on the pH-turbidity relation of PM*: At pH's far removed from their isoelectric point, the PM vesicles bear a net electric charge, and long-range electrostatic repulsions are important in retarding aggregation. Consequently, increasing the $\Gamma/2$, which increases ionic shielding against electrostatic repulsions, would be expected to accelerate aggregation and lead to increased turbidity at a given pH and time of observation. The operation of this mechanism has already been demonstrated above for NaCl, $CaCl_2$, and $MgCl_2$ at pH 8.2; it is also clear from Fig. 8 at pH > 5. But changes in the pH-turbidity profile induced by altering $\Gamma/2$ also point to the presence of electrostatic *attractions* between PM vesicles.

Figs. 8 and 10 represent the remarkable finding that increasing the $\Gamma/2$ at the isoelectric pH decreases the fractional absorbance increment. The effect is dramatic, since $\Delta = 2.00$ for $\Gamma/2 = 0.001$ at 5 min and $\Delta = 0.20$ for $\Gamma/2 = 1.0$ at the same time. (In this latter case, one must also consider the fact that n_o has increased to 1.344, which tends to decrease Δ somewhat.) Addition of salt 30 min *after* lowering the pH leads to a decrease in absorbance over a period of hours, indicating reversal of aggregation. These facts can be explained when it is appreciated that the isoelectric point is simply the pH at which the net charge on the particles—and hence the long-range electrostatic repulsion between the particles—is minimal, permitting close approach. It is precisely under such conditions that short-range electrostatic forces, such as mosaic attractions (which require fairly specific geometric alignment), can become expressed. It is also possible that suitable charge mosaics are attained only after a certain fraction of the surface groups has become titrated. In any event, the extent of attraction between charge mosaics will be diminished by increasing $\Gamma/2$.

Approach to the isoelectric point will also lead to increasing charge fluctuation attractions (21), which are maximal at the pK's of the dissociable groups which engender them. These forces will also be suppressed by increasing $\Gamma/2$.

Increasing $\Gamma/2$ also lowers the isoelectric point slightly (to about pH 3.4), presumably because of negative cation absorption (32) and/or increased acid strength of some dissociable groups on external PM surfaces. Similar, but much larger, shifts of isoelectric point have been observed upon

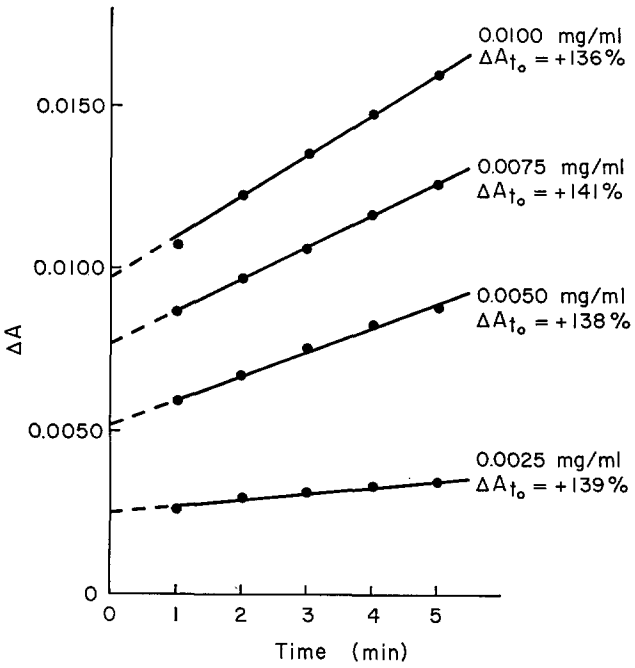

FIGURE 11 Increase of absorbance of ER suspensions of varying particle concentrations at various time intervals after reduction of pH from 8.2 to 4.35. ΔA is absolute change in absorbance at 400 mμ per cm optical path. Particle concentration is in terms of membrane protein. The fractional absorbance increment (in %) is given for each particle concentration.

addition of salts to dispersions of certain viruses (33) and phosphatides (34, 35).

Since changes in pH cause important alterations in vesicle geometry, quantitative evaluation of light-scattering and aggregation mechanisms is difficult. However, it appears that aggregation is much greater near the isoelectric point at low $\Gamma/2$ than upon addition of Ca^{2+} or Mg^{2+} under "standard conditions."

b. *ER vesicles.* i) *pH-Turbidity profile*: The variation of the turbidity of ER is given in Fig. 8 *b* for conditions identical to those for PM in Fig. 8 *a* ($\Gamma/2$ = 0.01 and 0.110, absorbance read 30 min after mixing). The absorbance of ER rises continuously between pH 7 and 4.35 ± 0.15, the presumptive isoelectric point. The absorbance declines abruptly as the hydrogen ion concentration is further increased; it is 50% lower at pH 2 than at pH 8.2.

The increase of turbidity between pH 7.0 and 4.35 (and its decline below pH 4.35) is only partly due to aggregation. This is brought out in Fig. 11, which shows the variation of absorbance with time following reduction of pH from 8.2 to 4.35 at very low particle concentration and at $\Gamma/2$ = 0.01. These measurements were obtained with 10-cm cuvettes.

It is evident that pH reduction produces an "instantaneous" rise in absorbance, followed by a further increase which is linear with time but which deviates from the concentration dependence expected from Equation 21 at concentrations above 0.005 mg/ml. Extrapolation of these kinetic curves to zero time shows that the transition from pH 8.2 to 4.35 produces an instantaneous absorbance increment of Δ = 1.38 ± 0.02 which is independent of particle concentration and is, therefore, believed to be structural, i.e. to reflect alterations of refractive index. More than 50% of the absorbance increment seen ½ hour after reduction of pH to 4.35 is structural.

Since ER suspensions show such large, concentration-independent absorbance changes, it is possible to obtain the pH-turbidity profile under conditions in which the effects of aggregation are excluded. This type of study is illustrated in Fig. 12. A 10-cm cuvette was employed. The ER concentration was 0.0046 mg protein per ml. Time-dependent absorbance changes (between pH 6 and 3.5) were extrapolated to zero time.

The pH-turbidity profile obtained in this manner is quite similar to that found when the contributions of aggregation to turbidity are included (Fig. 8 *b*). The maximal structural absorbance increment occurs at pH 4.35, which is also the pH for maximum aggregation. Below

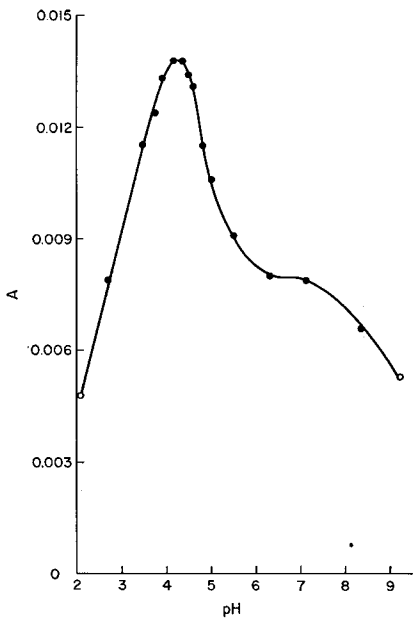

FIGURE 12 Absorbance of very dilute suspensions of ER vesicles at various levels of pH. λ is 400 mμ. Particle concentration is 0.0046 mg protein per ml. Time-dependent absorbance changes were extrapolated to time zero. Turbidity measurements were made with a 10-cm optical path but are presented as absorbance per cm light path.

pH 4.35, the structural effects decline strikingly, as does aggregation. The results suggest either that titration of dissociable groups on external ER surfaces is also responsible for structural changes, or that there are groups with similar pK's at both external and internal sites.

All of the above data are in accord with preliminary studies indicating that the maximum density of ER vesicles occurs at about pH 4.5. Moreover, the magnitude of the structural absorbance change and the difference in density between pH 8.2 and 4.5 (about 0.045 g/cc) can both be explained by deformation of the vesicles in the isoelectric region.

ii) *Effect of Γ/2 on the pH-turbidity relation of ER*: Neutral, uni-univalent salts decrease the extent and rate of absorbance change initiated by pH reduction to a degree depending upon ionic concentration. This phenomenon is illustrated for the case of NaCl in Fig. 8 *b*. Time- and concentration-dependent absorbance changes are virtually abolished by 0.1 M NaCl, leaving a structural absorbance increment at pH 4.35 of $\Delta = 1.60$, somewhat higher than at lower Γ/2. It thus appears that, just as in the case of PM, aggregation of ER vesicles in the isoelectric region is hindered by salt. However, since aggregation contributes less to the turbidity of ER than to that of PM, the effects of Γ/2 upon turbidity are not so dramatic in the case of ER as in the case of PM.

It should be noted that, also at pH levels away from the isoelectric point, the absorbance of ER is appreciably higher at $\Gamma/2 = 0.11$ than $\Gamma/2 = 0.01$. This effect of Γ/2, which is not related to aggregation, has been discussed above and is believed due to extrusion of water from ER vesicles at higher salt concentration, with resulting increase of density and relative refractive index.

GENERAL DISCUSSION

We conceive of the average PM vesicle under standard conditions as consisting of a spherical shell 85 A thick, with an outer radius of 717 A and a refractive index relative to water of 1.16. However, these average parameters are subject to experimental uncertainty. For example, the long extrapolation necessary to estimate n_2, the index of refraction of the wall, may be in error by as much as ±1%. Such an error could lead to a variation of ∓6% in the average outer radius. Similarly, our error in the estimation of the median value of ρ_w, the hydrated wall density, is ±0.5%, giving an error of ∓4% in β, the volume fraction of the wall, and ∓10% in the average external radius.

A second weakness of our model is that it seeks to describe a heterogeneous group of particles in terms of a few average parameters. We again wish to emphasize that the PM fraction is a population of membrane fragments which are similar in composition, over-all organization, and many physicochemical properties, but which, nonetheless, show considerable enzymatic and immunologic diversity (15). This heterogeneity of the PM fraction is also seen in some of our density measurements. Thus, equilibration of PM in glycerol-density gradients reveals a broad distribution of hydrated wall densities under standard conditions (15), with median and weight-average values of 1.150 and 1.160, respectively, and a standard deviation (SD) of 0.017. If we assume that all PM vesicles have a constant total density, $\rho_p = 1.045$, then variation in ρ_w of ±2 SD implies variation in external radius of approximately ∓200 A. Actually, however, the particles also manifest

some variation in ρ_p, the SD being about 0.007. But particles whose ρ_p is larger than average have values of ρ_w which are also larger than average. Consequently, the population's range in particle radius is smaller than the $\mp$200 A estimated above. Our model does, therefore, faithfully represent a sizeable fraction of the PM particle population and also serves as a convenient and useful heuristic device.

We also inquire to what extent the artefactitious PM vesicles provide information relevant to the surface properties of intact EAC. In this regard, it is reassuring to find that the outer surfaces of PM vesicles titrate over the same range of pH as the surface of the intact cell, and that the isoelectric points of the two coincide closely. But our experiments also show that on the alkaline side of the isoelectric point the major density increase of PM vesicles occurs between pH 6.5 and 4.5, whereas the major reduction of surface potential, inferred either from turbidity measurements or from electrophoresis of whole cells (27–30), occurs between pH 5 and 3.6. Whereas the surface potential is determined primarily by the net charge on the external surfaces of the vesicles, the total particle density depends also upon the ionic properties of the internal surface. Therefore, one would expect alterations in surface potential and total density to occur *pari passu* only when the ionogenic groups on the internal and external charge regions of the PM wall titrate over the same pH range. Since this was not observed, we conclude that the plasma membrane has distinctive inner and outer surfaces (i.e., is dissymmetric). This view that plasma membrane is dissymmetric is also consistent with studies on whole cells, such as the electron-microscope observations of Sjöstrand (36) and Doggenweiler and Frenk (37), and the established fact that the inner and outer surfaces of erythrocyte ghosts have different sensitivities to Na^+ and K^+, respectively (38). We conclude, therefore, that the PM fraction is composed, in large part, of pieces of surface membrane which have resealed, after cell rupture, to form vesicles with the orientation of the original membrane, and that this orientation is dissymmetric.

Just the reverse conclusion applies to the ER vesicles. Here we find that structural changes and alterations of surface potential occur over the same range of pH. Thus, no dissymmetry can be inferred involving the ionic properties of the inner and outer surfaces of ER vesicles. This view, which is also supported by electron-microscope observations (36, 37), is not intended to imply that the internal and external surfaces of ER are identical in all respects, but it is a strong argument against the simple unitarian view (39) that endoplasmic reticulum and plasma membrane are the same membrane material, differing only in location.

Our experiments provide the information that PM (and to a lesser extent ER) surfaces exhibit significant net electrostatic attraction when near their isoelectric point, but are electrostatically repelled at pH levels far from the isoelectric region. This change from net electrostatic attraction to net repulsion could mean that the mechanisms of electrostatic attraction exist only near the isoelectric pH. This would be so in the case of charge fluctuation attractions involving carboxyl groups. On the other hand, attractions between charge mosaics may very well operate also at physiological pH, but may escape detection in our present system because of the large, long-range electrostatic repulsion at pH levels far from the isoelectric point. Mosaic attractions may represent biologically important and even sterically specific mechanisms of interaction between cells under physiological conditions.

In this connection, we wish to point out that EAC are highly "malignant" cells and that such cells typically exhibit anomalous intercellular relationships, including abnormally low mutual adhesiveness (40). The apparent lack of electrostatic attraction between PM vesicles at pH levels away from the isoelectric point may thus represent a peculiarity of the malignant cell surface. It is clearly essential to examine the electrostatic properties also of membranes derived from normal or less malignant cells.

It is well known that the structural integrity of ribosomes and their reversible association with the endoplasmic reticulum depends dramatically on magnesium concentration. Our experiments show that Mg^{2+} (and Ca^{2+}) produce a much larger density increase (5, 15) and aggregation-independent fractional absorbance increment in the ribosome-free ER vesicles than in PM. Clearly the structure of ER membranes, like that of ribosomes, is very sensitive to alkaline earth ions, while that of PM is not. It remains to be determined to what extent this phenomenon is related to the nonribosomal RNA which is tightly associated with ER, but not PM membranes (41).

The experiments presented here do not provide information about the permeability properties of

PM and ER vesicles. We have previously reported on this topic (4, 14) and have shown that these particles have restricted permeabilities even to small, uncharged molecules. Studies on the turbidities of liver microsomes in media of differing osmotic activities but constant refractive index lead to a similar conclusion (42).

This work was aided by grant CA 07382 from the United States Public Health Service. Dr. Wallach is a Fellow of the Leukemia Society. Mr. Gail was supported by grant 5 T5 GM 51-05 from United States Public Health Service.

Received for publication 28 February 1966.

REFERENCES

1. WALLACH, D. F. H., and EYLAR, E. H., *Biochim. et Biophysica Acta*, 1961, **52,** 594.
2. WALLACH, D. F. H., and HAGER, E. B., *Nature*, 1962, **96,** 1004.
3. WALLACH, D. F. H., and ULLREY, D., *Biochim. et Biophysica Acta*, 1964, **88,** 620.
4. WALLACH, D. F. H., and KAMAT, V. B., *Proc. Nat. Acad. Sc.*, 1964, **52,** 721.
5. KAMAT, V. B., and WALLACH, D. F. H., *Science*, 1965, **148,** 1343.
6. WALLACH, D. F. H., and KAMAT, V. B., *Methods Enzymol.*, in press.
7. MOORE, S., and STEIN, W. H., *J. Biol. Chem.*, 1948, **176,** 367.
8. LORD, RALEIGH, *Phil. Mag.*, 1881, **12,** 81.
9. MIE, G., *Ann. Physik*, 1908, **25,** 377.
10. JÖBST, G., *Ann. Physik*, 1925, **78,** 157.
11. KOCH, A. L., *Biochim. et Biophysica Acta*, 1961, **51,** 429.
12. HELLER, W., and PANGONIS, W. J., *J. Chem. Phys.*, 1957, **26,** 498.
13. KERKER, M., KRATHOVIL, J. P., and MATIJEVIC, E., *J. Opt. Soc. Am.*, 1962, **52,** 551.
14. WALLACH, D. F. H., KAMAT, V. B., and MURPHY, F. L., Symposium on Mechanisms of Invasiveness in Cancer, International Union Against Cancer, July 1965, Paris, in press.
15. WALLACH, D. F. H., Symposium on the Specificity of Cell Surfaces, Society of General Physiologists, Woods Hole, September, 1965, in press.
16. THOMPSON, T. E., *in* Cellular Membranes in Development, (M. Locke, editor), New York, Academic Press Inc., 1964.
17. ROBERTSON, J. D., and WALLACH, D. F. H., unpublished observations.
18. VANDENHEUVEL, F. A., *J. Am. Oil Chemists Society*, 1963, **40,** 455.
19. DAVIES, J. T., and RIDEAL, E. K., Interfacial Phenomena, New York, Academic Press Inc., 1961.
20. PETHICA, B. A., *Exp. Cell Research*, 1961, suppl. **8,** 123.
21. KIRKWOOD, J. G., and SHUMAKER, J. B., *Proc. Nat. Acad. Sc.*, 1952, **38,** 863.
22. BIERMAN, A., *J. Colloid Sc.*, 1955, **10,** 231.
23. LOEB, A. L., *J. Colloid Sc.*, 1951, **6,** 75.
24. THOMPSON, T. E., and MCLEES, B. D., *Biochim. et Biophysica Acta*, 1961, **50,** 213.
25. OSTER, G., *J. Colloid Sc.*, 1947, **2,** 291.
26. OVERBEEK, J. TH. G., *in* Colloid Science, (H. R. Kruyt, editor), Amsterdam, Elsevier, 1949, **1,** 310.
27. STRAUMFJORD, J. V., JR., and HUMMEL, J. P., *Cancer Research*, 1959, **19,** 913.
28. BANGHAM, A. D., and PETHICA, B. A., *Proc. Roy. Phys. Soc. Edinburgh*, 1960, **28,** 43.
29. BANGHAM, A. D., GLOVER, J. C., HOLLINGSHEAD, S. and PETHICA, B. A., *Biochem. J.*, 1962, **84,** 513.
30. COOK, G. M. W., HEARD, D. H., and SEAMAN, G. V. F., *Exp. Cell Research*, 1962, **28,** 27.
31. LUCY, J. A., *J. Theoret. Biol.*, 1964, **7,** 360.
32. HAYDON, D. A., *Biochim. et Biophysica Acta*, 1961, **50,** 457.
33. OSTER, G., *J. Biol. Chem.*, 1951, **190,** 55.
34. ABRAMSON, M. B., KATZMAN, R., and GREGOR, H. P., *J. Biol. Chem.*, 1964, **239,** 70.
35. ABRAMSON, M. B., KATZMAN, R., WILSON, C. E., and GREGOR, H. P., *J. Biol. Chem.*, 1964, **239,** 4066.
36. SJÖSTRAND, F. S., *J. Ultrastruct. Research*, 1963, **8,** 517.
37. DOGGENWEILER, C. F., and FRENK, S., *Proc. Nat. Acad. Sc.*, 1965, **53,** No. 2, 425.
38. WHITTAM, R., and AGER, M. E., *Biochem. J.*, 1964, **93,** 337.
39. ROBERTSON, J. D., *Biochem. Soc. Symp.*, 1959, **16,** 1.
40. ABERCROMBIE, M., and AMBROSE, E. J., *Cancer Research*, 1962, **22,** 525.
41. ZAHLER, P. H., and WALLACH, D. F. H., data to be published.
42. TEDESCHI, H., JAMES, J. M., and ANTHONY, W., *J. Cell Biol.*, 1963, **18,** 503.